THE ASTROPHYSICAL JOURNAL, 277:51–63, 1984 February 1

OBSERVATIONS OF THREE QSOs WITH COMPLEX, BROAD ABSORPTION LINES[1]

D. A. TURNSHEK[2] AND R. J. WEYMANN
Steward Observatory, University of Arizona

R. F. CARSWELL
Institute of Astronomy, Cambridge University

AND

M. G. SMITH
Royal Observatory, Edinburgh

Received 1983 February 4; accepted 1983 July 22

ABSTRACT

We present spectroscopy of three QSOs with complex, high-ionization absorption. The QSOs belong to the broad absorption-line class of QSOs and exhibit absorption troughs with considerable structure (i.e., the absorption is not the classical P Cygni type). We discuss the nature of the broad absorption by considering the consequences of the generally accepted models for the broad emission-line region. We show that the broad absorption-line clouds are incapable of giving rise to all of the observed broad emission lines, particularly Mg II. Therefore, if the broad absorption-line region gives rise to observable emission, the generally adopted (optically thick, single component) models for the emission-line region are incorrect. A two (or more) component model for the broad emission/absorption-line region cannot be ruled out. A high-ionization, outer component could conceivably give rise to broad absorption lines and some broad high-ionization emission lines. Alternatively, the broad absorption-line region may not give rise to appreciable emission. It may lie well beyond, and be separate and distinct from, the broad emission-line region.

Subject headings: line formation — quasars

I. INTRODUCTION

We present spectroscopic observations of three QSOs exhibiting complex, high-ionization absorption. The objects studied have intrinsic absorption characteristics placing them in the class of QSOs referred to as broad absorption-line (BAL) QSOs. Weymann, Carswell, and Smith (1981) have discussed the criteria which must be considered when trying to decide if a QSO should be placed in this class. Other similar-quality (i.e., high resolution, high signal-to-noise ratio) observations of BAL QSOs have been presented by Boksenberg *et al.* (1978), Clowes *et al.* (1979), Turnshek *et al.* (1980), Shaver, Boksenberg, and Robertson (1982), Turnshek and Weymann (1984), and Foltz *et al.* (1983*a*, *b*). A summary of the properties of BAL QSOs is given in Turnshek (1984*b*). The importance of this class of objects is apparent when one considers that between 3% and 10% of all moderate-to-high redshift QSOs are observed to have BALs, and that the BAL region is likely to cover only a small fraction ($\lesssim 20\%$) of the central source (cf. Turnshek *et al.* 1980). That is, a substantial fraction of QSOs must have BAL regions which are not observable via a broad absorption signature.

The main purpose here is to present good-quality spectroscopic observations of this somewhat neglected, but important, class of QSOs. This is done in § II. The BAL profiles of the objects studied here are complex in that substantial velocity structure is apparent in the troughs. With the exception of PHL 5200, RS 23, and H1413+113 (cf. Turnshek and Weymann 1984), the other BAL QSOs that have been well studied to date also tend to have BAL profiles which are complex. PHL 5200, RS 23, and H1413+113 have fairly smooth, P Cygni–like BAL profiles.

In § III we discuss the absorption expected when the types of clouds thought to be responsible for the observed broad emission lines occult the continuum source. We try to decide if broad emission-line clouds can cause the BALs. Some of the observations presented in § II are particularly well suited for application to this problem. We find that if the broad emission-line region (BELR) is composed solely of numerous, individually optically thick clouds with highly ionized front surfaces, then the emitting clouds cannot give rise to the BALs. Likewise, the BAL clouds are shown to be incapable of accounting for all of the observed emission lines, particularly Mg II λ2798. Therefore, if the BAL clouds do give rise to observable emission, the generally adopted (optically thick, single component) models for the BELR must be incorrect. Some implications of this deduction are discussed in Turnshek (1984*a*). Other interpretive results are discussed in Scott, Christiansen, and Weymann (1984) and Turnshek (1984*c*).

II. OBSERVATIONS

The equipment used to gather the spectroscopic data is summarized in Table 1. In each case the observations were made in one of four possible modes. Red observations were made with a Reticon on the Steward Observatory 2.3 m telescope. For these observations the Steward Reticon was lens-coupled to a four-stage Varo image tube and attached to a modified Boller and Chivens spectrograph (Hege, Cromwell, and Woolf 1979). The grating used yielded a resolution of

[1] The research reported here is based in part upon data acquired at the MMT Observatory and the AAT Observatory. The MMTO is a joint facility of the University of Arizona and the Smithsonian Institution.

[2] Also, Department of Physics and Astronomy, University of Pittsburgh.

TABLE 1

JOURNAL OF OBSERVATIONS

Object	Date	Exp. Time (min)	Resolution (Å)	Mode[a]	Fig.
Q0932+501	1980 May	60	~2.5	2	1
Q0932+501	1980 May	100	~10	1	2
Q1303+308	1978 Jun (Plate 2565)	125	~2	3	3
Q1303+308	1978 Jun (Plate 2587)	120	~2	3	3
Q1303+308	1979 May (Plate 2871)	120	~2	3	3
Q1303+308	1980 Mar (Plate 2906)	120	~2	3	3
Q1303+308	1981 May	30	~10	2	4
Q1303+308	1979 Mar	50	~10	1	5
Q1303+308	1980 May	100	~10	1	5
Q1309−056	1979 Apr	120	~2	4	6
Q1309−056	1979 Mar	50	~10	1	7
Q1309−056	1980 May	50	~10	1	7

[a] (1) Steward Observatory 2.3 m and Reticon. (2) MMT and Reticon. (3) Steward Observatory 2.3 m and photographic plates. (4) AAT and IPCS.

8–10 Å. Blue observations utilized either N_2-baked IIa-O plates on the Steward Observatory 2.3 m telescope or the University College London Image Photon Counting Spectrometer (IPCS) on the 3.9 m Anglo-Australian Telescope. In the first case, the photographic plates were lens-coupled to an RCA image tube on a modified Boller and Chivens spectrograph. The plate density was converted to an intensity scale using a PDS microdensitometer and an average density-to-intensity relation. The IPCS is described by Boksenberg (1972). Both blue systems yielded a resolution of about 2 Å. The last mode utilized the Smithsonian Astrophysical Observatory Reticon and the Multiple Mirror Telescope Spectrograph on the Multiple Mirror Telescope (4.5 m). The SAO Reticon is fiber optically coupled to a Varo image tube. The particular gratings used yielded resolutions of approximately 2.5 or 10 Å. Note that the sky and tube noise have not been subtracted from the photographic data but have been subtracted from the digital data. The photographic data for Q1303+308 have been normalized and represent a co-addition of four plates. The gross features in this spectrum were normalized by forcing agreement over 200 Å running averages. The digital data have been put on a relative flux scale using standard star observations. Below we give a description of the spectrum of each object. The emission-line redshifts are given in Table 2; Tables 3–5 give the absorption-line data for each of the three objects.

a) Q0932+501

This QSO was discovered by Notni, Kauachentsev, and Afanasjev (1979) during a search for radio-quiet ultraviolet-excess objects. Notni *et al.* report the blue magnitude as 17.4, but our observations indicate that it is somewhat brighter than this (~17). The spectra we present of Q0932+501 are a MMT scan near C IV λ1549 (4000–5000 Å) at a resolution of 2.5 Å (Fig. 1) and a single 2.3 m scan in the red (4100–7200 Å) at a resolution of 10 Å (Fig. 2). C III] λ1909 emission appears to be broader (full width of 23,000 km s^{-1}) than C IV λ1549 emission. This may be due to contamination of C III] by Al III λ1857 emission and/or Fe II emission (cf. Wills *et al.* 1980). In addition, the emission near C III] is stronger than the C IV emission. The emission redshift derived from C III] (Table 2) is 1.88.

As was the convention in Turnshek *et al.* (1980), uppercase letters are used to denote entire absorption troughs, and lowercase letters are used to denote individual "sharp"

TABLE 2

EMISSION REDSHIFTS

Object	C III] λ1909	Redshift
Q0932+501[a]	5500 Å	1.88 ± 0.01
Q1303+308	5267 Å	1.759 ± 0.005
Q1309−056[a]	6110 Å	2.20 ± 0.01

[a] C III] is extremely broad. The velocities at full width are ~±20,000 km s^{-1}.

TABLE 3

Q0932+501 ABSORPTION FEATURES

A. MEASUREMENTS

Feature	λ_{obs} (Å)	Suggested Identification	Redshift	Notes
a	5260	Al III $\lambda\lambda$1854.7, 1862.8	1.832	1
b	5150	Al III $\lambda\lambda$1854.7, 1862.8	1.773	2
A2 (rd)	4415	C IV λ1550.8	1.847	
c	4400	C IV $\lambda\lambda$1548.2, 1550.8	1.839	1
d	4360	C IV $\lambda\lambda$1548.2, 1550.8	1.814	
e	4306	C IV $\lambda\lambda$1548.2, 1550.8	1.779	2
f	4273	C IV $\lambda\lambda$1548.2, 1550.8	1.758	
A1 (bl)	4239	C IV λ1548.2	1.738	

B. PREDICTED ABSORPTION TROUGH WAVELENGTHS (Å)

Feature	Al III
A2 (rd)	5303
A1 (bl)	5078

NOTES.—(1) The absorption line is broad (~1700 km s^{-1}, $\Delta z_{abs} = 0.015$). The lower ionization material (Al III) appears to be in the high-velocity cloudlets which make up the absorption line. (2) The absorption line is broad (~3300 km s^{-1}, $\Delta z_{abs} = 0.026$). The lower ionization material (Al III) appears to be in the higher velocity cloudlets which make up the absorption line.

TABLE 4

Q1303+308 ABSORPTION FEATURES

A. MEASUREMENTS

Feature	λ_{obs} (Å)	Suggested Identification(s)	Redshift(s)	Notes
a	4304.0	C IV λ1550.8	1.7754	
b	4297.6	C IV λ1548.2	1.7759	
A3 (rd)	4289	C IV λ1550.8	1.766	
c	4284.6	C IV λ1550.8	1.7628	
d	4277.0	C IV λ1548.2	1.7626	
e	4267.2	... (C IV λ1550.8)	... (1.7516)	
f	4258.0	C IV λ1550.8 (C IV λ1548.2)	1.7457 (1.7503)	1
g	4250.8	C IV λ1548.2	1.7456	
h	4229.0	C IV (C IV λ1550.8)	1.729 (1.7232)	2
i	4216.0	... (C IV λ1548.2)	... (1.7232)	
j	4197.2	C IV $\lambda\lambda$1550.8, 1548.2	1.709	3
k	4168.8	C IV	1.691	4
A2 (bl)	4154	C IV λ1548.2	1.683	
l	4142.2	C IV 1550.8	1.6710	
m	4134.8	C IV λ1548.2(C IV λ1550.8?)	1.6707 (1.6659)	
n	4127.4	C IV λ1550.8 (C IV λ1548.2?)	1.6615 (1.6662)	
o	4120.6	C IV λ1548.2	1.6615	
A1 (bl)	4115	C IV λ1548.2	1.658	
B2 (rd)	4046	C IV λ1550.8	1.609	
p	4038.0	C IV $\lambda\lambda$1550.8, 1548.2	1.607	3
q	4022.0	C IV $\lambda\lambda$1550.8, 1548.2	1.596	3
B1 (bl)	4015	C IV λ1548.2	1.593	
C2 (rd)	3955	C IV λ1550.8	1.550	
r	3944.0	C IV $\lambda\lambda$1550.8, 1548.2	1.546	3
C1 (bl)	3936	C IV λ1548.2	1.542	
s	3875.8	Si IV λ1402.8	1.7629	
t	3850.8	Si IV λ1393.8 (Si IV λ1402.8)	1.7628 (1.7451)	5
u	3826.8	Si IV λ1402.8 (Si IV λ1393.8)	1.7280 (1.7456)	5
v	3802.6	Si IV λ1393.8 (Si IV λ1402.8)	1.7282 (1.7107)	5
w	3773.8	Si IV λ1402.8 (Si IV λ1393.8)	1.6902 (1.7076)	5
x	3748.2	Si IV λ1393.8	1.6892	5
y	3658.0	C IV λ1550.8	1.3588	
z	3652.4	C IV λ1548.2	1.3591	
a′	3438.0	N V λ1238.8	1.7753	
b′	3434.0	N V λ1242.8	1.7631	
c′	3422.0	N V λ1238.8	1.7624	
d′	3412.0	N V λ1242.8	1.7454	
e′	3401.0	N V λ1238.8	1.7454	
f′	3391.2	N V λ1242.8	1.7287	
g′	3381.4	N V λ1238.8	1.7296:	6
h′	3373.2	N V λ1238.8	1.7230	
i′	3364.8	N V λ1242.8	1.7074	
j′	3354.6	N V λ1238.8	1.7079	
k′	3336.0	N V $\lambda\lambda$1242.8, 1238.8	1.690	3
l′	3306.0	N V $\lambda\lambda$1238.8, 1242.8	1.666	3
m′	3267.0	Lyα λ1216?	1.687	7

B. PREDICTED ABSORPTION TROUGH WAVELENGTHS (Å)

Feature	Lyα	N V	Si IV	Mg II
A3 (rd)	3363	3454	3880	7753
A2 (bl)	3262	3323	3740	7502
A1 (bl)	3232	3293	3705	7432
B2 (rd)	...	...	3660	7313
B1 (bl)	...	...	3614	7250
C2 (rd)	...	...	3577	7148
C1 (bl)	...	...	3543	7107

NOTES.—(1) The λ1548.2 feature produces the red asymmetry on feature f. (2) This is a suspected blend of three lines: $\lambda\lambda$1550.8, 1548.2 with $z_{abs} = 1.729$ and λ1550.8 with $z_{abs} = 1.7232$. (3) This is a suspected broad C IV doublet. (4) This is suspected to be a blend of two C IV doublets or possibly a single broad C IV doublet. (5) Features s through x are five overlapping (i.e., absorption-absorption line locked) Si IV doublets. Features u through x exhibit broad structure in the line "wings." These wings are not damping wings. They are due to velocity structure and the sometimes inexact overlapping. Since the measurements of wavelength pertain to the line centers, this inexact overlapping sometimes produces absorption redshift discrepancies which are not real (e.g., doublet vw). (6) This is a blend with the λ1242.8 line corresponding to feature h′. (7) This broad feature may be Lyα corresponding to feature k (C IV), wx (Si IV), and k′ (N V). Blending may be confusing the determination of z_{abs}.

TABLE 5

Q1309−056 Absorption Features

A. Measurements

Feature	λ_{obs} (Å)	EW (Å)	Suggested Identification(s)	Redshift(s)	Notes
A2 (rd)	4913	...	C IV λ1550.8	2.168	
a	4905.6	5.0	C IV λ1550.8	2.1633	1
b	4897.6	6.2	C IV λ1548.2 (C IV λ1550.8)	1.1634 (2.1581)	1
c	4889.4	3.9	C IV λ1550.8 (C IV λ1548.2)	2.1528 (2.1581)	1
d	4880.8	1.6	C IV λ1548.2	2.1526	1
A1 (bl)	4876	...	C IV λ1548.2	2.149	
e	4859.5	1.5	C IV λ1550.8	2.1335	
f	4850.8	2.1	C IV λ1548.2	2.1332	
B3 (rd)	4749	...	C IV λ1548.2	2.067	
g	4742.7	2.6	C IV λ1550.8	2.0582	
h	4734.1	2.1	C IV λ1548.2	2.0578	
i	4717.0	12.6	C IV λλ1550.8, 1548.8	2.045	2
B2 (bl)	4607	...	C IV λ1548.2	1.976	
B1 (bl)	4476	...	C IV λ1548.2	1.891	
j	4438.1	2.3	Si IV λ1402.8	2.1637	
k	4409.8	2.4	Si IV λ1393.8	2.1638	
l	4393.1	...	...	...	
m	4270.3	2.8	Si IV λ1402.8	2.0441	
n	4243.0	3.0	Si IV λ1393.8	2.0442	
o	3932.1	2.6	N V λ1242.8	2.1639	
p	3925.0	1.8	N V λ1242.8	2.1585	
q	3918.6	3.8	N V λ1238.8	2.1632	
r	3912.8	2.6	N V λ1238.8	2.1585	
s	3905.9	1.3	N V λ1238.8	2.1530	3
t	3897.8	0.3	...	...	
u	3869.8	0.3	...	...	
v	3855.2	0.4	...	...	
w	3848.5	0.7	Lyα λ1215.7	2.1656	4
x	3844.4	1.0	Lyα λ1215.7	2.1623	4
y	3836.0	1.4	Lyα λ1215.7	2.1554	4
z	3809.2	4.4	Lyα λ1215.7	2.1333	
a′	3799.0	1.7	...	2.0568	
b′	3792.2	1.6	...	...	
c′	3784.8	5.4	N V λ1242.8	2.0454	
d′	3772.4	3.5	N V λ1238.8	2.0452	
e′	3699.6	3.2	Lyα λ1215.7	2.0432	5
f′	3673.1	2.0	...	...	
g′	3655.0	3.2	...	...	
h′	3639.1	3.4	...	1.9376	
i′	3632.5	1.7	...	...	
j′	3613.2	1.3	...	1.9073	
k′	3601.1	2.4	...	1.9069	

B. Predicted Absorption Trough Wavelengths (Å)

Feature	Lyα	N V	Si IV
A2 (rd)	3851	3937	4444
A1 (bl)	3829	4390	4389
B3 (rd)	3723	3809	4296
B2 (bl)	3618	3686	4148
B1 (bl)	3515	3581	4030

Notes.—(1) Features a through d are three overlapping (i.e., absorption-absorption line locked) C IV doublets. The existence of three components is verified by the N V absorption. (2) This is a suspected broad C IV doublet. (3) The λ1242.8 member of feature s is blended with feature q. (4) These are the Lyα lines corresponding to the absorption complex between A2 (rd) and A1 (bl). Features w and x may correspond to the single lines in C IV (features a, b), Si IV (features j, k), and N V (features o, q). The fact that w and x do not appear as a single line may be due to velocity structure or noise. However, in general, the agreement does not appear to be perfect, e.g., Lyα (feature y), C IV (features b, c and/or c, d), N V (features p, r and/or s, q:). (5) The identification of feature e′ is tentative since there is imperfect agreement with Si IV (features m, n) and N V (features c′, d′).

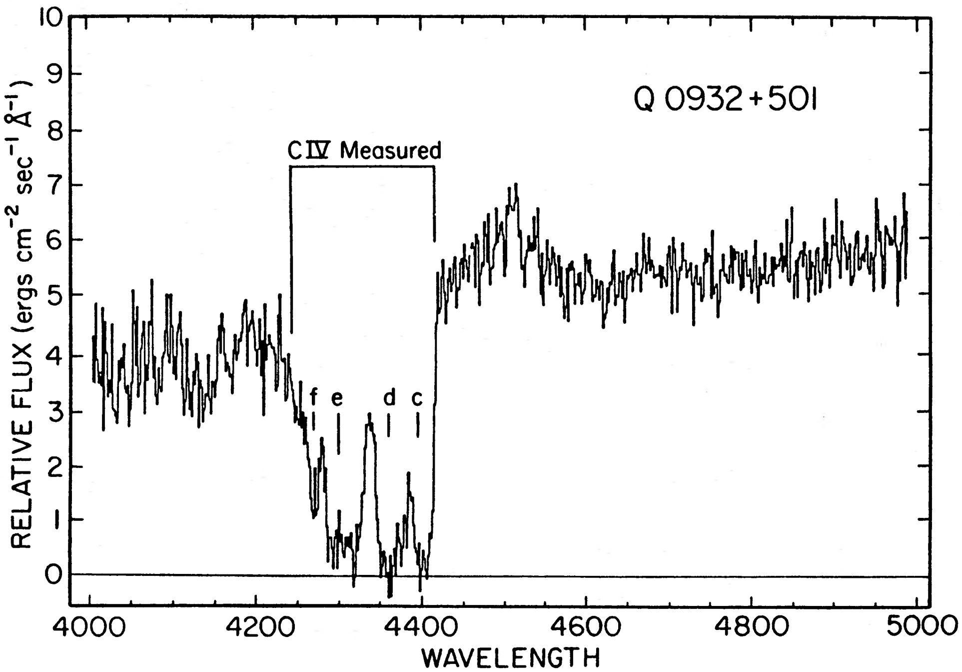

FIG. 1.—2.5 Å resolution Reticon spectrum of Q0932+501 taken at the MMT

features. The numeral following uppercase letters designates the portion of the trough that was measured. In Q0932+501 we have used C IV $\lambda\lambda$1548.2, 1550.8 to measure a single detached absorption trough (4500–16,200 km s^{-1}, Table 3). There is considerable absorption structure in the trough, and we attribute this to clouds (having a range of velocities) occulting the continuum source. Notni *et al.* suggested that the structure in the absorption trough represents narrow emission peaks, originating in shocks which develop between the QSO's wind and intergalactic material. This view is almost certainly incorrect since there are cases where similar structure in an absorption trough is a natural consequence of the doublet separation (e.g., Q1303+308, this study). In addition to C IV absorption (and also Si IV and N V absorption reported by Notni *et al.*), there is also absorption due to Al III $\lambda\lambda$1854.7, 1862.8. In Figure 2 features a and b (both unresolved Al III doublets) correspond to features c and e (both blended C IV doublets). However, there is no Al III feature corresponding to the strong feature d (C IV). In both cases where Al III is identified, the lower ionization material (Al III)

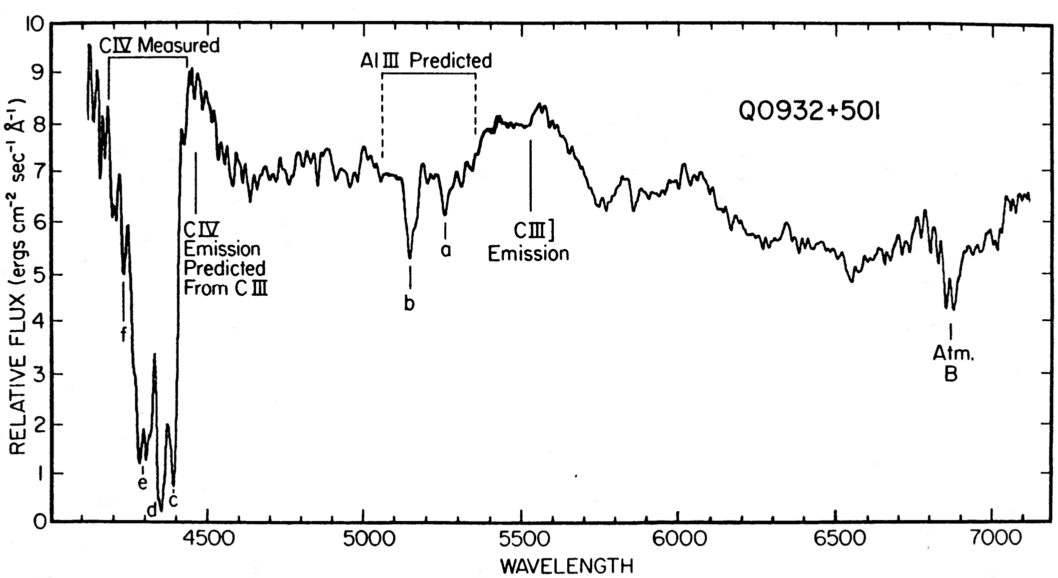

FIG. 2.—10 Å resolution red Reticon spectrum of Q0932+501 taken at the 2.3 m

appears to be the most dominant in the high-velocity cloudlets which make up the absorption systems as defined by C IV measurements.

b) *Q1303+308*

Q1303+308 is W22722 (Weistrop 1973) and PB 3296 (Berger and Fringant 1977). It was originally selected on the basis of color, having a blue magnitude of $\sim$17.9 (Weistrop 1973). This is one of the two QSOs Weymann *et al.* (1979) specified as having intrinsic absorption. The spectra we present are a co-addition of four 2.3 m blue photographic spectra (3200–4400 Å) at a resolution of 2 Å (Fig. 3), a moderately red MMT scan at a resolution of 10 Å (Fig. 4), and a co-addition of two 2.3 m red scans (4600–7900 Å) at a resolution of 10 Å (Fig. 5). C III] λ1909 emission appears broad (full width of $\sim$20,000 km s^{-1}) and is apparently much stronger than C IV λ1549 emission (although the strength of C IV emission may be reduced by absorption; see Fig. 4). The emission redshift from C III] is 1.759.

Using C IV $\lambda\lambda$1548.2, 1550.8 (Table 4), we have denoted trough A (-760 to 11,190 km s^{-1}), trough B (16,760–18,600 km s^{-1}), and trough C (23,590–24,520 km s^{-1}). However, calling A an absorption "trough" is somewhat superficial in view of the many individual doublets that are identifiable. Also, the only basis for identifying absorption troughs B and C as due to C IV results from the fact that they fall between the C IV and Si IV + [O IV] emission lines; any other identification would be ad hoc. Other notable features in the spectra are (i) the lack of low-ionization Mg II $\lambda\lambda$2795.5, 2802.7 broad absorption, (ii) the presence of five overlapping Si IV $\lambda\lambda$1393.8, 1402.8 doublets corresponding to trough A, and (iii) the presence of strong high-ionization N V $\lambda\lambda$1238.8, 1242.8 doublets corresponding to trough A. Also present is a narrow, highly displaced C IV $\lambda\lambda$1548.2, 1550.8 doublet (feature zy).

c) *Q1309−056*

This QSO was discovered on objective prism plates by Osmer and Smith (1977). They list the blue magnitude as 17.0. The spectra we present are a blue scan (3500–5100 Å) having a resolution of 2 Å (Fig. 6) and a co-addition of two red scans (4500–7700 Å) having a resolution of 10 Å (Fig. 7). The lower curve in Figure 6 gives the estimate of the noise. As is the case with Q0932+501, C III] λ1909 emission *appears* to be stronger and broader (full width of $\sim$34,000 km s^{-1}) than C IV λ1549 emission. Lyα emission appears to be very weak or absent (the majority of the emission at λ3930 is probably due to N V rather than Lyα). The emission redshift derived from C III] is 2.20 (Table 2).

We make the following identifications in the C IV $\lambda\lambda$1548.2, 1550.8 region: trough A (3020–4820 km s^{-1}) is formed by three overlapping doublets, feature fe (6310 km s^{-1}) is a single, narrow doublet, and trough B (12,730–30,360 km s^{-1}) has smooth, continuous absorption (at our resolution) as well as an individual doublet and other absorption structure. Trough A exhibits moderate to weak Lyα and Si IV absorption and strong N V absorption; corresponding to trough B is moderate Si IV absorption and strong N V absorption (the strength of Lyα absorption being indeterminate because of the presence of N V absorption). There are no additional absorption lines corresponding to feature fe.

III. ANALYSIS AND DISCUSSION

In this observational investigation we consider only two topics concerning the BAL QSO phenomenon. More thorough discussions of the astrophysical implications of BAL QSOs

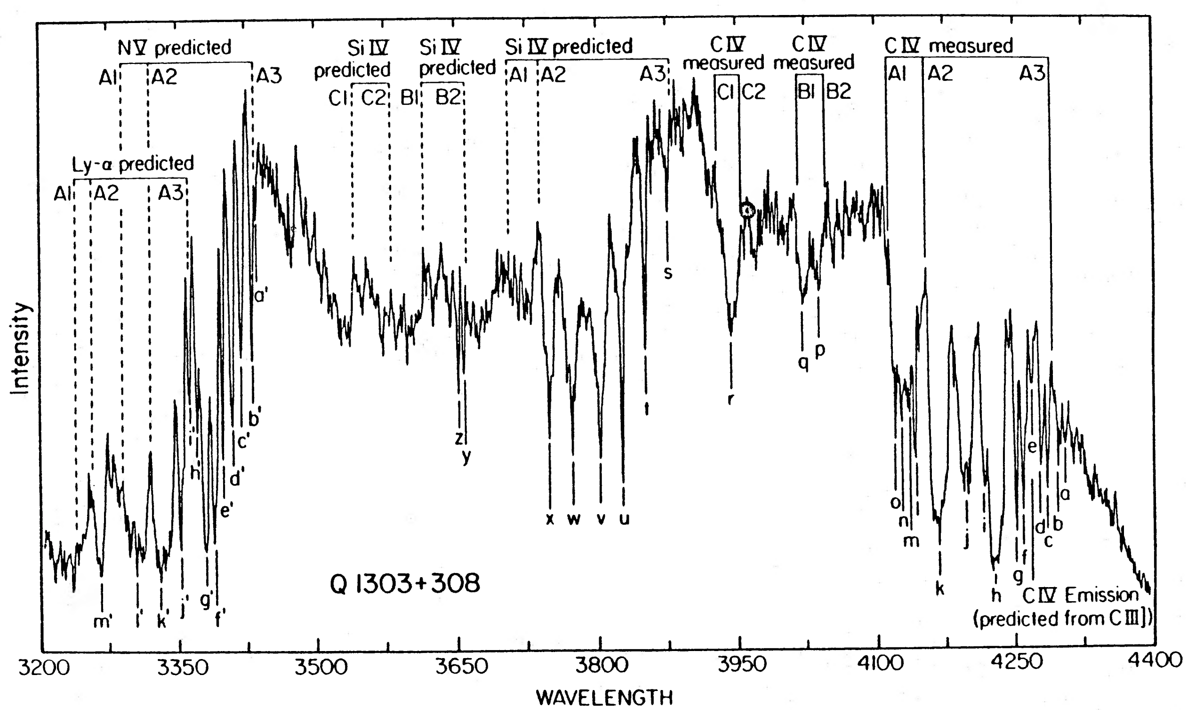

FIG. 3.—2 Å resolution blue photographic spectrum of Q1303+308 taken at the 2.3 m

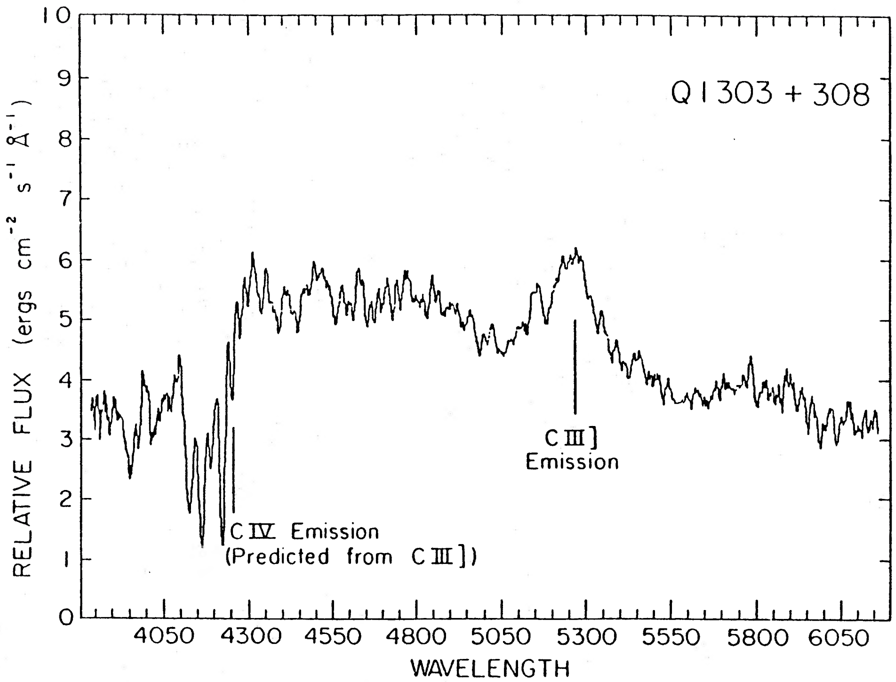

FIG. 4.—10 Å resolution Reticon spectrum of Q1303+308 taken at the MMT

can be found elsewhere (cf. Turnshek 1981; Weymann, Carswell, and Smith 1981; Scott, Christiansen, and Weymann 1984; Turnshek 1984*a*, *b*, *c*). First, we contrast the absorption characteristics of these particular objects with other members of the BAL class and summarize some inferences which may be drawn from the observations. Second, we discuss the nature of the BALs by quantifying one of the strongest arguments for believing that the BALs are not due to the same clouds producing the (low ionization) broad emission lines in the generally accepted photoionization models for the BELR.

a) *Contrasts with Other Objects and Inferences*

BAL profiles come in many varieties. At one extreme are the BAL QSOs with P Cygni–like profiles. They include PHL 5200, RS 23, and H1413+113 (Turnshek and Weymann 1984). Their absorption troughs appear to be fairly smooth. At the other extreme is a BAL QSO which shows little evidence for smooth absorption but rather has individual absorption lines. This is Q1303+308, which is studied here. The remaining BAL QSOs generally have absorption characteristics which

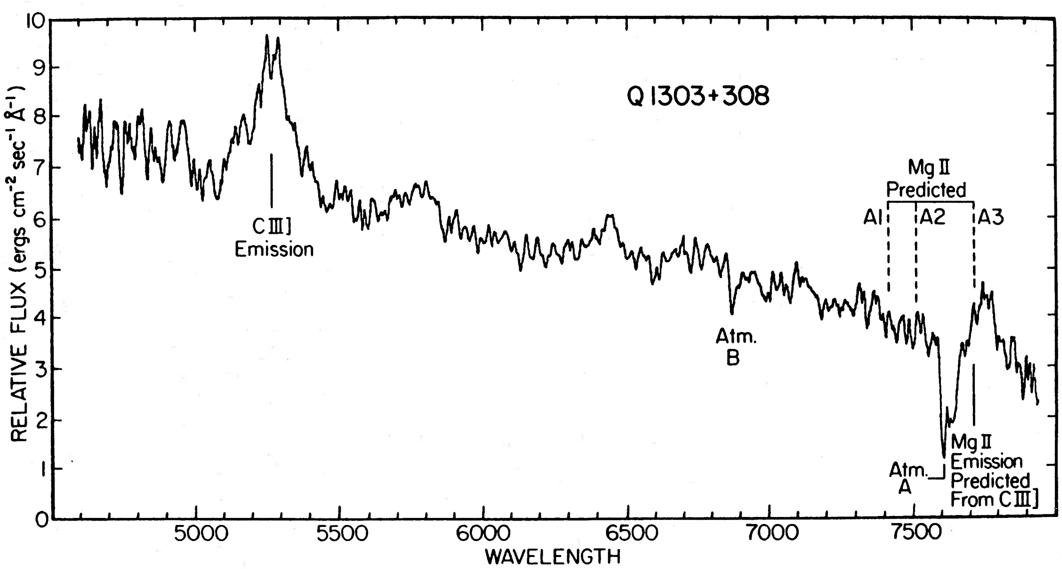

FIG. 5.—10 Å resolution red Reticon spectrum of Q1303+308 taken at the 2.3 m

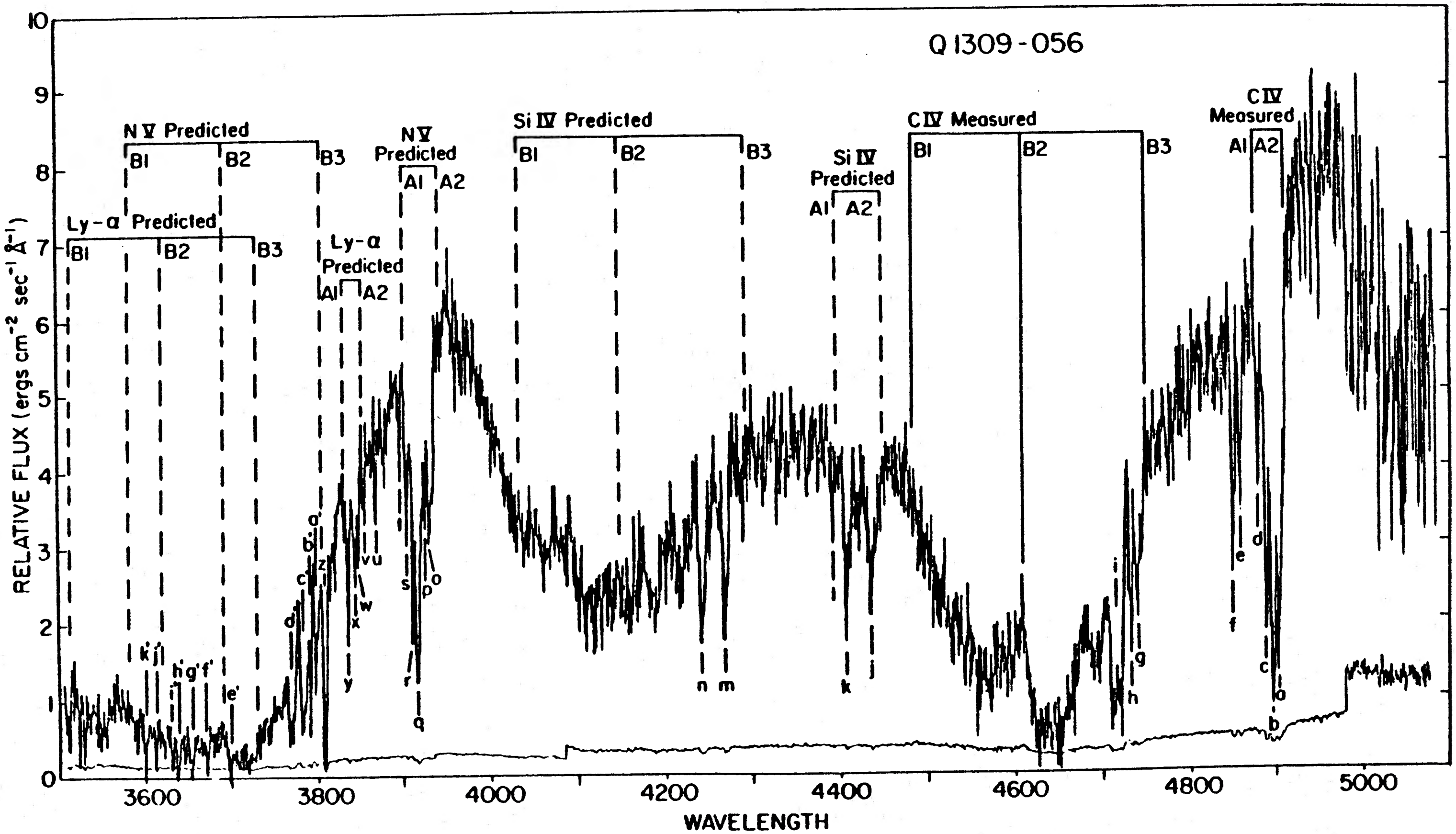

FIG. 6.—2 Å resolution IPCS spectrum of Q1309−056 taken at the AAT

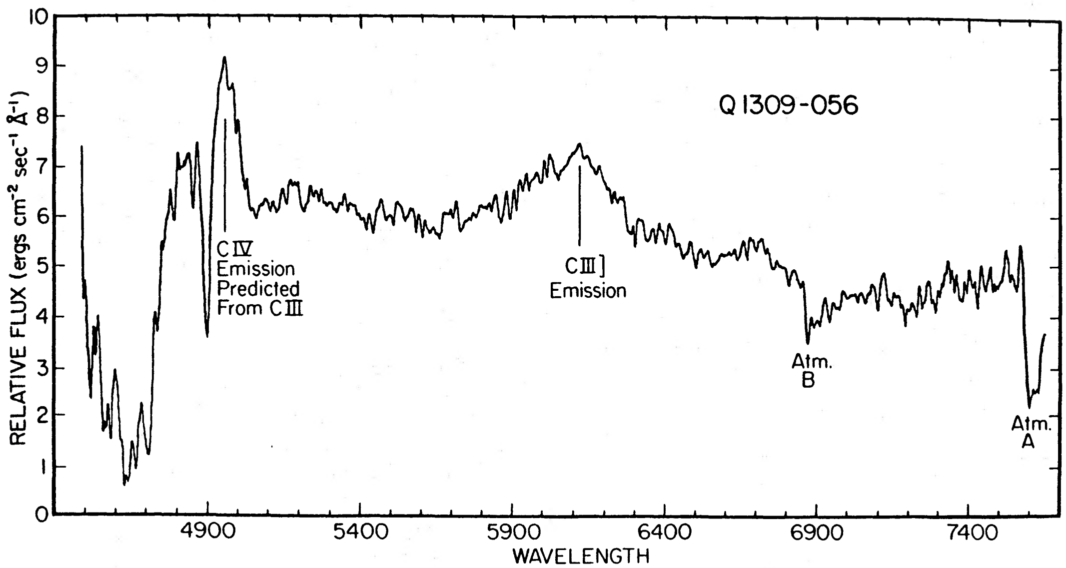

FIG. 7.—10 Å resolution red Reticon spectrum of Q1309−056 taken at the 2.3 m

are intermediate between these two extremes. Often observed are detached absorption troughs, multiple absorption troughs, and individual absorption lines. Q0932+501 and Q1309−056 both fit into this intermediate (perhaps more typical) category.

It is this variety that has prompted us to comment in the past that we may be observing an evolutionary sequence (Weymann *et al.* 1979; Turnshek *et al.* 1980). In this scenario BAL QSOs with P Cygni profiles would exemplify the youngest type of absorbing region, eventually evolving into a Q1303+308 type object as the absorbing clouds became older and more spread out or as instabilities broke up an initially smooth flow. Another possibility is that the BAL material is distributed in a rather preferential manner with respect to the central source (e.g., a disk geometry). If this is the case, the absorption profile might depend on aspect angle (e.g., the scale height of the line of sight passing through a disk). See Turnshek (1984*c*) and Scott *et al.* for some additional discussion. Each situation (and possibly a combination of the two) deserves future consideration.

Last, when absorption doublets are observed in many BAL profiles, they are often overlapping in velocity space. A good example of this for C IV $\lambda\lambda$1548.2, 1550.8 is found in the spectrum of Q1309−056 (trough A in Fig. 6); good examples of this for Si IV $\lambda\lambda$1393.8, 1402.8 are found in the spectra of MCS 275 (Turnshek *et al.* 1980) and Q1303+308 (Fig. 3). See also the absorption-line lists for these three objects. Presumably, this is absorption-absorption line-locking, which can be induced by radiation pressure (e.g., Scargle 1973).

b) Absorption from Emitting Clouds

In the past, various investigators have discussed models in which the clouds responsible for the BALs were also responsible for the broad emission lines. The most notable of these is the P Cygni–like model, which suggests that redshifted emission lines are formed adjacent to blueshifted absorption by resonance line scattering in an expanding envelope surrounding the optical continuum source (e.g., Scargle, Caroff, and Noerdlinger 1970). Although we believe this particular view to be largely incorrect (Turnshek *et al.* 1980), it is important to explore the constraints on any model which proposes that BALs are observable when the clouds responsible for the broad emission lines cover the continuum source.

Photoionization models of the BELR generally require the individual clouds to be optically thick in the Lyman continuum so that Mg II λ2798 emission can be produced. Since highly ionized species are also observed (e.g., C IV), the individual emission-line clouds are normally modeled to have a highly ionized front surface, where C IV λ1549 is produced by collisional excitation, followed by a transition zone (and somewhat of a neutral region), where Mg II is produced by collisional excitation. (Such a single-component model for the BELR is especially attractive when trying to explain cases where the broad emission-line profiles are approximately similar for different ionic species.) The emission-line clouds are thought to intercept 3% to 10% of the continuum radiation (cf. Baldwin and Netzer 1978; Smith *et al.* 1981). The lower limit of 3% is the typical value obtained when the ionizing continuum is taken to be the observed continuum (extrapolated beyond the Lyman limit) and approximately one-half of the observed Lyα emission is taken to be due to recombination. The upper limit of 10% is assigned because, statistically, less than one in 10 QSOs have a Lyman edge corresponding to $z_{\rm em}$. (However, note that there are no cases where the emission-line clouds can unambiguously be interpreted to cause an observed Lyman edge.) To some extent, the latter estimate is based on the assumption that an individual emission-line cloud is capable of covering a significant fraction of the continuum source. In view of the (perhaps likely) possibility that individual emission-line clouds are numerous and very small when compared with the size of the continuum source (cf. McKee and Tarter 1975; Blumenthal and Mathews 1979), we note that the upper limit of 10% is also consistent with a Lyman edge produced by many small clouds covering less than 10% of the source.

We now consider the relevance of the following possible coincidence: the fraction of QSOs with BALs is similarly estimated to be 3% to 10% (Hazard *et al.* 1984). In view of this (and the general possibility of broad emission-line clouds covering the central continuum source), it is important to decide if the properties of the BAL clouds are consistent with emission-line clouds covering the continuum source. Recently, Kwan and Krolik (1981) discussed a model of the BELR which has the general properties outlined above. The calculation is moderately successful at explaining the hydrogen line ratios in QSOs. The model supposes that the optical depths are large enough to thermalize the Lyα photons; i.e., a significant fraction of the hydrogen is in excited states, thereby allowing mainly collisional excitation to enhance the Balmer lines (whereas Lyα becomes saturated). A substantial electron fraction is maintained throughout each optically thick cloud since photoionization and collisional ionization from excited states of hydrogen are included in the model. Soft X-ray photoionization of helium and metals also contributes to collisional heating of the gas in this region. Kwan and Krolik point out that, in addition to the hydrogen lines, the normally observed lines such as Mg II, Si IV, C IV, N V, and O VI are optically thick. The optical depths for Si IV, C IV, N V, and O VI are small enough that, although a photon created in an emission-line cloud will be scattered many times, the photon generally escapes before being destroyed. However, a limitation is imposed on the growth of Mg II λ2798 emission by collisional de-excitation and by bound-free absorption of λ2798 from the $n = 2$ level of hydrogen. In view of these properties (i.e., large optical depths in the resonance lines), it seems at least plausible that broad absorption lines might be present in objects having emission-line clouds covering the continuum source.

In order to delineate the constraints on such a situation, we first deduce the column densities of ground-state C^{+3} and Mg^{+1} ions in emission-line clouds that are modeled to be *optically thick with highly ionized front surfaces.* We then show that these theoretical emission-line cloud column densities are inconsistent with the observed column densities of BAL clouds, suggesting that either (i) our adopted model for the BELR is incorrect, or (ii) the clouds causing the BALs are not (alone) capable of causing all (or any) of the observed emission lines.

i) *Column Densities of Emitting Clouds*

We utilize the model of Kwan and Krolik (1981). They adopt a carbon abundance of ∼57% of the solar value, require the clouds to be in pressure equilibrium, and take the continuum to be a smooth two-component power law with

$$\begin{aligned} L_\nu &\sim \nu^{-0.5}\,, \quad h\nu \lesssim 13.6 \text{ eV}\,; \\ &\sim \nu^{-2}\,, \quad 13.6 \text{ eV} \lesssim h\nu \lesssim 100 \text{ eV}\,; \\ &\sim \nu^{-0.5}\,, \quad 100 \text{ eV} \lesssim h\nu\,. \end{aligned} \tag{1}$$

They terminate their standard model at a total column density of 10^{23} cm^{-2}, at which point the calculated emission-line flux ratio of C IV to Mg II is ∼3.7. This lies in the quoted "observed" range of 1.0–4.4 given by Kwan and Krolik. See also Baldwin (1975, 1977), Osmer and Smith (1976, 1977), Grandi and Phillips (1979), Neugebauer *et al.* (1979), Shuder and MacAlpine (1979), Green *et al.* (1980), and Wu, Boggess, and Gull (1980) for a relevant discussion of the observations.

We deduce the column densities graphically by using Figures 2 and 3 of Kwan and Krolik (1981). This is done by numerically solving the integral

$$N_i = \int_r^{r+\Delta r} n_i \, dr \tag{2}$$

with statistical equilibrium requiring

$$n_i = \frac{j_i}{n_e q_{12} h\nu_i}\left(1 + \frac{\omega_1}{\omega_2}\frac{n_e q_{12}}{A_{21} p}\right) \exp\left(+\frac{h\nu_i}{kT}\right). \tag{3}$$

Here, N_i is the column density of *ground-state* ions (for ion i), n_i is the corresponding number density, r is the radial location of the cloud, Δr is the effective radial extent of the cloud, j_i is the emissivity (caused by collisional excitation), n_e is the electron density, q_{12} is the rate of collisional excitation (cf. Osterbrock and Wallace 1977), $h\nu_i$ is the energy of the transition, ω_1 and ω_2 are the statistical weights of the lower and upper levels, $A_{21}p$ is the effective rate of spontaneous emission, T is the electron temperature, and k is the Boltzmann constant. In particular, the variable p is the escape probability of a line photon, and when p becomes small, e.g.,

$$p \lesssim 10 \frac{\omega_1}{\omega_2}\frac{n_e q_{12}}{A_{21}} \exp\left(+\frac{h\nu_i}{kT}\right) \tag{4}$$

(i.e., when the optical depth in the line is large), collisional de-excitation can occur. As noted previously, this effect is not very important for C IV (reducing the emission by ∼10% at any one point in the cloud), but it is more important for Mg II. Far more important for Mg II, however, is the destruction of Mg II photons by Balmer-continuum absorption. The total Balmer-continuum optical depth is $\tau_B \approx 0.86$, and as a result of the effect of repeated scatterings, caused by large Mg II line center optical depths ($\tau_{\rm Mg\,II} \approx 10^6$), only an average of $\exp[-5\tau_B(\nu)^{0.75}] \approx 6\%$ of the Mg II emission escapes the cloud (cf. Bonilha *et al.* 1979; Hummer and Kunasz 1980). We adopt $p = 0.9$ for C IV and $p = 0.05$ for Mg II as a first-order estimate. We report the deduced column densities and line center optical depths for the BELR clouds in Table 6. The Mg II to C IV column density ratio is found to be ∼5. Note that the line center optical depths ($\tau_{\lambda 2795} \approx 2 \times 10^6$, $\tau_{\lambda 1548} \approx 3 \times 10^4$) are so large in part because the clouds have been taken to be only thermally broadened [i.e., $(v_D)_{\rm Mg\,II} \approx 2.2$ km s^{-1}, $(v_D)_{\rm C\,IV} \approx 5.2$ km s^{-1}]. Emitting clouds having large turbulent velocities, v_D, would have reduced line center optical depths since

$$\tau_{\rm line} \approx \frac{\sqrt{\pi}}{v_D}\frac{e^2}{m_e c} N f \lambda\,. \tag{5}$$

This, in turn, would eliminate the reduction in emission due to collisional de-excitation, as well as limit the destruction of Mg II λ2798 by Balmer-continuum absorption. The net result would be more emission (especially for Mg II) for the parameters adopted by Kwan and Krolik (1981). Since Mg II is produced throughout the cloud, Mg II emission could be reduced by making the Mg II column densities smaller. However, adopting a large Doppler parameter would, in general, reduce the radiative transfer effects (which give the proper hydrogen line intensities) sought after by Kwan and Krolik (1981).

TABLE 6

COLUMN DENSITIES IN EMITTING AND ABSORBING CLOUDS

Parameter	Model of Kwan and Krolik (Emission)[a]	Simplified Model (Emission) Case 1[b]	Case 2[c]	Fit to Observations (Absorption)
$N_{\rm C\,IV}$ (cm^{-2})	4×10^{17}	3×10^{17}	3×10^{17}	$\gtrsim 4.1 \times 10^{15}$
$N_{\rm Mg\,II}$ (cm^{-2})	2×10^{18}	8×10^{17}	8×10^{17}	$\lesssim 1.1 \times 10^{14}$
τ_{1548}	3×10^4	2.4×10^4	5.0×10^2	$\gtrsim 0.5$
τ_{2795}	2×10^6	7.4×10^5	7.4×10^3	...
$(v_{\rm D})_{\rm C\,IV}$ (km s^{-1})	5.2	5.2	250	250–700
$(v_{\rm D})_{\rm Mg\,II}$ (km s^{-1})	2.2	2.5	250	250–700
$N_{\rm Mg\,II}/N_{\rm C\,IV}$	5	3	3	$\lesssim 2.7 \times 10^{-2}$

[a] The model of Kwan and Krolik 1981 is described in the text.

[b] $v_{\rm D} = (v_{\rm D})_{\rm thermal}$.

[c] $v_{\rm D} = (v_{\rm D})_{\rm turbulent}$.

In order to gauge the effects of a large Doppler parameter, the column densities for a second, simplified model for the emitting clouds have been deduced. We assume that all of the C IV emission is produced in a region with $T \sim 20{,}000$ K and $n_e \sim 4 \times 10^9$ cm^3, and that all of the Mg II λ2798 emission is produced in a region with $T \sim 10{,}000$ K and $n_e \sim 4 \times 10^8$ cm^3. This is somewhat of a compromise between models by MacAlpine (1972), Davidson (1972), and Kwan and Krolik (1981). We ignore any collisional de-excitation and loss of Mg II emission caused by Balmer-continuum absorption. The Doppler parameter is taken to be both the thermal value and 250 km s^{-1} (designated case 1 and 2, respectively, in Table 6). As before, we adopt the flux ratio of C IV to Mg II to be $\sim$3.7; we also assume that the flux emitted by a column through the emitting cloud (ergs s^{-1} cm^{-2}) is the same as that emitted by the clouds of Kwan and Krolik. The results are reported in Table 6 along with the results for the Kwan and Krolik clouds.

The main point of this simplified calculation for optically thick emission-line clouds is to demonstrate that the line center optical depths will be much greater than unity for reasonable values of $v_{\rm D}$. (Even $v_{\rm D} \approx 250$ km s^{-1} may be unrealistically high.) Furthermore, there is no way to significantly reduce the column densities quoted in Table 6. This is because the size of the ionized region is roughly given by balancing ionizations with the effective number of recombinations:

$$\int_{\nu_0}^{\infty} \frac{L_\nu}{h\nu}\, d\nu \approx \frac{n_e^{\,2}}{1.4}\, \beta 4\pi r^2 \Delta r_{\rm H\,II}\,, \tag{6}$$

where $L_\nu \sim \nu^{-\alpha}$ is the QSO luminosity (ν_0 corresponding to the Lyman edge), r is the distance between the continuum source and the emitting cloud, $\Delta r_{\rm H\,II}$ is the effective extent of the ionized region (with $\Delta r_{\rm H\,II}/r \ll 1$), and β is the effective rate of recombination to the excited states. This yields

$$\Delta r_{\rm H\,II} \approx \frac{1.4 L_{\nu_0}}{n_e^{\,2} \beta 4\pi r^2 h\alpha}\,, \tag{7}$$

or, since the photoionization parameter ($\xi = L_{\nu_0}/n_e r^2$) is presumably fixed by the observations,

$$\Delta r_{\rm H\,II} \approx \frac{1.4\xi}{n_e \beta 4\pi h\alpha}\,. \tag{8}$$

Thus, the column density of C IV (for example) must be

$$N_{\rm C\,IV} \approx \Delta r_{\rm H\,II}\, n_{\rm C\,IV}\,, \tag{9}$$

$$N_{\rm C\,IV} \approx \frac{1.4\xi}{\beta 4\pi h\alpha} \frac{n_{\rm C\,IV}}{n_e}\,, \tag{10}$$

where $n_{\rm C\,IV} = (n_{\rm C\,IV}/n_{\rm C})(n_{\rm C}/n_{\rm H})(n_e/1.4)$. Therefore,

$$N_{\rm C\,IV} \approx \frac{\xi}{\beta 4\pi h\alpha} \frac{n_{\rm C\,IV}}{n_{\rm C}} \frac{n_{\rm C}}{n_{\rm H}} \approx 10^{18} \tag{11}$$

for typical BELR values [e.g., $\log\ \xi = -16.4$, $\alpha = 2$, $(n_{\rm C\,IV}/n_{\rm C}) = 0.3$, and $(n_{\rm C}/n_{\rm H}) = 3.3 \times 10^{-4}$].

ii) *Column Densities of Absorbing Clouds*

We have used Q1303+308 observations to put an *upper limit* on the Mg II to C IV column density ratio in the broad absorption-line clouds. This was accomplished by fitting a theoretical profile of clouds having turbulent velocities of $v_{\rm D} \approx 250$–700 km s^{-1} to the observed C IV BAL profile of features a through o (Fig. 3). Note that these values for $v_{\rm D}$ are likely to be conceptually meaningless in the classical sense. The sky and tube noise were estimated and removed from the C IV region before the fit was made by utilizing a moderate-resolution, low signal-to-noise Reticon scan with the Steward Observatory 2.3 m telescope (not shown). Since the observed absorption lines are somewhat saturated, the resultant theoretical profile yields a lower limit for the C IV column density responsible for features r through o. This is because we did not increase the C IV column density past the point of obtaining a reasonable fit. That is, the C IV column density could have been higher without destroying the fit. An *upper limit* for the Mg II column density was found using the same technique and requiring the theoretical profile to be consistent with the signal-to-noise ratio (Fig. 5). The number of velocity-broadened absorbing clouds, $v_{\rm D}$, and $N_{\rm Mg\,II}/N_{\rm C\,IV}$ were kept constant. Unfortunately, the presence of the atmospheric A band near Mg II prohibited us from using the lower velocity portions of the absorption in the analysis. The theoretical profiles were degraded to the instrumental resolution for both C IV and Mg II. This degradation had little effect on the resultant C IV profile since the resolution was $\sim$140 km s^{-1} in the cloud rest frame. The effect was more pronounced for Mg II, where the resolution was $\sim$400 km s^{-1} in the cloud rest frame. We stress that this procedure truly produces a *lower limit* on the ratio of C IV to Mg II column densities since, in principle, the C IV column density could be larger because of saturation, and the Mg II column density could be considerably smaller. The final fits used in the determination of column densities are shown in Figure 8. The deduced properties of the Q1303+308 broad absorbing clouds are included in Table 6.

iii) *Deductions*

As can be seen from Table 6, $(N_{\mathrm{Mg\,II}}/N_{\mathrm{C\,IV}})_{\mathrm{em}} \lesssim 100 \times (N_{\mathrm{Mg\,II}}/N_{\mathrm{C\,IV}})_{\mathrm{abs}}$. This disagreement between the ratio of Mg II to C IV column density in the model for emitting clouds versus the absorbing clouds requires us to conclude that *the BALs could not be due to the types of clouds generally adopted to produce a QSO's broad emission-line spectrum.* In addition to the lack of Mg II BALs in Q1303+308, this result is supported by several other observations. First, PHL 5200 (see Junkkarinen, Burbidge, and Smith 1983 for the spectrum) also lacks appreciable Mg II absorption. A similar analysis shows that the same degree of disagreement exists in that case. Note that Mg II is weakly present in some other BAL QSOs. However, owing to the weakness of Mg II in these objects, our arguments still apply. Second, MCS 141 (Turnshek *et al.* 1980) and Q0932+501 (*IUE* observations by Turnshek and Turnshek 1984) lack a Lyman edge corresponding to the broad absorption. If optically thick emission-line clouds with highly ionized front surfaces obscured the entire continuum source, thereby causing deep BALs, we would expect to see absorption at the Lyman edge of an absorption trough. For example, Kwan and Krolik (1981) predict $\tau_{912} \approx 10^5$–10^6. Third, it is generally true that the strength of Lyα broad absorption is weak, almost never rivaling C IV λ1549 broad absorption, and it is sometimes weaker than Si IV λ1397. However, the models of Kwan and Krolik (1981) and others predicted substantial Lyα optical depths. See Q1246−057 (Boksenberg *et al.* 1978), MCS 232, MCS 275, MCS 141 (Turnshek *et al.* 1980), and Q1309−056 (Fig. 6) for some examples of the weakness of Lyα broad absorption relative to C IV broad absorption. Last, we note that some of the observed C IV doublets in the broad absorption troughs are not saturated, having $\tau_{\mathrm{line}} \lesssim 2$ (e.g., Q1303+308 and Q1309−056, § II). From equation (5) we find that this is not in accord with the optically thick clouds normally proposed for the BELR (see Table 6).

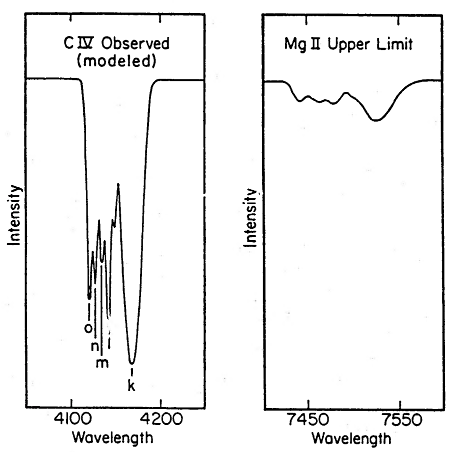

FIG. 8.—Fit to C IV absorption and upper limit to Mg II absorption in Q1303+308.

Having pointed out the above problems, we must add to our initial comments concerning the similarity of the "covering factors" for the BELR and the BAL region. If the individual emission-line clouds really are *optically thick* and characterized by a *small Doppler parameter* $[v_{\mathrm{D}} \sim (v_{\mathrm{D}})_{\mathrm{thermal}}]$, we would not necessarily expect *broad* absorption lines to be observed as would be if the idealized case we have just considered held. For example, if an individual emission-line cloud occulted the entire central continuum source, we would expect to observe a *narrow* absorption line at z_{abs} less than z_{em} (for an outflow model). Only a single high-ionization absorption line would be present since clouds farther from the QSO (if they were present) would be shielded from ionizing photons by continuous absorption in the Lyman continuum (caused by the emission-line cloud nearest to the QSO along the line of sight). See, for example, Carswell and Ferland (1981). The absorption line would be so narrow that it would be filled-in even at moderately high resolution. If many individual emission-line clouds covered approximately 3% to 10% of the continuum source, there could be numerous narrow absorption lines overlapping in velocity space, perhaps giving the appearance of broad absorption. However, a doublet (e.g., C IV) would be saturated, and the absorption would not be deep as a result of insufficient source coverage (i.e., the central intensities would be no smaller than 0.9 of the continuum). Only if there were preferential large-scale clumping, so that at times many individual emission-line clouds covered approximately 100% of the source, would we actually expect deep, broad absorption lines from emission-line clouds. However, the broad absorption-line doublets (e.g., C IV) would always be saturated according to equations (5) and (11) [i.e., $v_{\mathrm{D}} \approx (v_{\mathrm{D}})_{\mathrm{thermal}}$], and this is not always observed. Of course, our initial result concerning the lack of strong Mg II BALs demonstrates the unsuitability of employing a single-component model for explaining the broad emission/broad absorption phenomenon in any case.

Owing to these considerations we can conclude with certainty that under no circumstances could a single-component model for the BELR produce BALs with the characteristics that have been observed. However, we cannot rule out the possibility that two-component or multi-component models for the BELR are relevant. In the past, multicomponent models for the BELR have been suggested by Netzer (1976), Davidson (1977), and Baldwin and Netzer (1978) because of the fact that the predicted amount of N V and O VI emission by single-component models is normally less than that observed. Kwan and Krolik (1981) also noted the possible importance of a multicomponent model for fitting the observations. However, the problems with N V and O VI strengths could also be related to abundances. Recently, Gaskell (1982), Wilkes and Carswell (1982), and Clavel *et al.* (1983) have discussed other evidence supporting separate low-ionization, optically thick components and high-ionization, optically thin components. We point out here that a high-ionization component in the BELR may be responsible for not only high-ionization emission but also the observed BALs (cf. Turnshek 1984*a*). However, since Lyα emission is often occulted by N V BALs (Turnshek 1984*b*), the high-ionization component would have to cover the low-ionization component. This geometry is contrary to the assumptions of past multicomponent models. In fact, multicomponent models which simply adopt a large enough range in surface photoionization parameters (yet still employ optically thick clouds with highly ionized front surfaces) are capable of eliminating the N V and O VI discrepancies, but could not produce the observed BALs. Alternatively, a model in which BAL material does not give rise to appreciable emission may be feasible. The BAL region may lie well beyond, and be separate and distinct from, the BELR.

REFERENCES

Baldwin, J. A. 1975, *Ap. J.*, **201**, 26.
———. 1977, *Ap. J.*, **214**, 679.
Baldwin, J. A., and Netzer, H. 1978, *Ap. J.*, **226**, 1.
Berger, J., and Fringant, A. 1977, *Astr. Ap. Suppl.*, **28**, 123.
Blumenthal, G. R., and Mathews, W. G. 1979, *Ap. J.*, **233**, 479.
Boksenberg, A. 1972, in *Proceedings of the ESO/CERN Conference on Auxiliary Instrumentation for Large Telescopes*, ed. S. Laustsen and A. Reiz (Geneva: ESO-Telescope Project Division CERN), p. 295.
Boksenberg, A., Carswell, R. F., Smith, M. G., and Whelan, J. A. J. 1978, *M.N.R.A.S.*, **184**, 773.
Bonihla, J. R. M., Ferch, R., Salpeter, E. E., Slater, G., and Noerdlinger, P. D. 1979, *Ap. J.*, **233**, 649.
Carswell, R. F., and Ferland, G. J. 1981, *M.N.R.A.S.*, **191**, 55.
Clavel, J., *et al.* 1983, *M.N.R.A.S.*, **202**, 85.
Clowes, R. G., Smith, M. G., Savage, A., Cannon, R. D., Boksenberg, A., and Wall, J. V. 1979, *M.N.R.A.S.*, **189**, 175.
Davidson, K. 1972, *Ap. J.*, **171**, 213.
———. 1977, *Ap. J.*, **218**, 20.
Foltz, C., Wilkes, B., Weymann, R., and Turnshek, D. 1983*a*, *Pub. A.S.P.*, **95**, 341.
———. 1983*b*, *Pub. A.S.P.*, submitted.
Gaskell, M. 1982, *Ap. J.*, **263**, 79.
Grandi, S. A., and Phillips, M. M. 1979, *Ap. J.*, **232**, 659.
Green, R. F., Pier, J. R., Schmidt, M., Estabrook, F. B., Lane, A. L., and Wahlquist, H. D. 1980, *Ap. J.*, **239**, 483.
Hazard, C., Terlevich, R., Morton, D., and McMahon, R. 1984, *M.N.R.A.S.*, submitted.
Hege, E. K., Cromwell, R. H., and Woolf, N. J. 1979, *Adv. Electronics Electron Phys.*, **52**, 397.
Hummer, D. G., and Kunasz, P. B. 1980, *Ap. J.*, **236**, 609.
Junkkarinen, V. T., Burbidge, E. M., and Smith, H. E. 1983, *Ap. J.*, **265**, 51.
Kwan, J., and Krolik, J. H. 1981, *Ap. J.*, **250**, 478.
MacAlpine, G. M. 1972, *Ap. J.*, **175**, 11.
McKee, C. F., and Tarter, C. B. 1975, *Ap. J.*, **202**, 306.
Netzer, H. 1976, *M.N.R.A.S.*, **177**, 473.
Neugebauer, G., Oke, J. B., Becklin, E. E., and Matthews, K. 1979, *Ap. J.*, **230**, 79.
Notni, P., Kauachentsev, I. D., and Afanasjev, V. L. 1979, *Astr. Nach.*, **300**, No. 3, p. 121.
Osmer, P. S., and Smith, M. G. 1976, *Ap. J.*, **210**, 267.
———. 1977, *Ap. J.*, **213**, 607.
Osterbrock, D. E., and Wallace, R. K. 1977, *Ap. Letters*, **19**, 11.
Scargle, J. D. 1973, *Ap. J.*, **179**, 705.
Scargle, J. D., Caroff, L. J., and Noerdlinger, P. D. 1970, *Ap. J.* (*Letters*), **161**, L115.
Scott, J. S., Christiansen, W. A., and Weymann, R. J. 1984, *Ap. J.*, in press.
Shaver, P. A., Boksenberg, A., and Robertson, J. G. 1982, *Ap. J.* (*Letters*), **262**, L7.
Shuder, J. M., and MacAlpine, G. M. 1979, *Ap. J.*, **230**, 348.
Smith, M. G., *et al.* 1981, *M.N.R.A.S.*, **195**, 437.
Turnshek, D. A. 1981, Ph.D. thesis, University of Arizona (available from University Microfilms, Inc., Ann Arbor, Mich.).
———. 1984*a*, *Ap. J.* (*Letters*), in press.
———. 1984*b*, *Ap. J.*, in press.
———. 1984*c*, *Ap. J.*, submitted.
Turnshek, D. A., and Turnshek, D. E. 1984, in preparation.
Turnshek, D. A., and Weymann, R. J. 1984, *Ap. J.*, submitted.
Turnshek, D. A., Weymann, R. J., Liebert, J. W., Williams, R. E., and Strittmatter, P. A. 1980, *Ap. J.*, **238**, 488.
Weistrop, D. 1973, *Astr. Ap.*, **23**, 215.
Weymann, R. J., Carswell, R. F., and Smith, M. G. 1981, *Ann. Rev. Astr. Ap.*, **19**, 41.
Weymann, R. J., Williams, R. E., Peterson, B. M., and Turnshek, D. A. 1979, *Ap. J.*, **234**, 33.
Wilkes, B., and Carswell, R. 1982, *M.N.R.A.S.*, **201**, 645.
Wills, B. J., Netzer, H., Uomoto, A. K., and Wills, D. 1980, *Ap. J.*, **237**, 319.
Wu, C., Boggess, A., and Gull, T. R. 1980, *Ap. J.*, **242**, 14.

R. F. CARSWELL: Institute of Astronomy, Cambridge University, Cambridge, England, UK

M. G. SMITH: Royal Observatory, Blackford Hill, Edinburgh, Scotland, UK

D. A. TURNSHEK: Department of Physics and Astronomy, University of Pittsburgh, Pittsburgh, PA 15260

R. J. WEYMANN: Steward Observatory, University of Arizona, Tucson, AZ 85721